Simulation and Exergy and Exergoeconomic Analysis of Associated Gas to Liquid Recovery Plant (Case Study: 4 and 5 Phases of South Pars)

Norouzi, Nima; Bashash Jafarabadi, Zahra; Valizadeh, Ghassem; Hemmati, Mohammad Hossein; Fani, Maryam*[+]

Department of Energy Engineering and Physics, Amirkabir University of Technology (Tehran Polytechnic), Tehran, I.R. IRAN

ABSTRACT: *In the last one hundred years, the increase in the use of fossil fuels in various industries, including refineries, petrochemicals, industrial complexes, etc., to achieve more production, has led to an increase in various pollutants in the world and environmental concerns, various economic costs, and health costs. Imposed on human beings. One of the most important sources of environmental pollution is industrial fluoride gases. According to global statistics, Iran is known as the third country to burn these gases. Reducing the emissions of these gases is one of the great goals of the international community. It seems necessary to study various methods such as converting gas to liquid to recover Flare gas. This research has simulated a gas-to-liquid conversion unit using the Flare gas output data of the south pars natural gas processing plant in Aspen Hysys V11 software. This unit is then evaluated and optimized by the exergy analysis method. The simulation output shows that when Flare gas is used to liquid the unit's raw material, 1549 barrels of gas to liquid products per day will be obtained from this unit. Investigation of this case shows that one of the appropriate solutions to recover Flare gas can be to create a gas to the liquid conversion unit with energy and exergy efficiency of 65% and 69%.*

KEYWORDS: *Exergy analysis; Flare gas; LNG; NGL; Flare management; Exergoeconomic.*

INTRODUCTION

Humans have always been and are one of the most important causes of harm to the environment. And they have negatively impacted the environment. This impact has become more and more profound in the last two centuries. It is the growth of industry and technology, the increase in population, and the growing needs and desires of human beings. Energy is the driving force of the industrial cycle and fossil fuels are the most important energy sources globally but are not renewable and nature-friendly sources. Since the mid-1970s, there was much work from the scientific society and governmental authorities to replace fossil fuels to prevent global warming and reduce environmental pollution. However, the use of fossil fuels is still the first place of consumption, and in Iran, due to its economic dependence on fossil fuels to move the country's industry and the cost of renewable energy sources,

* *To whom correspondence should be addressed.*
+ E-mail: mfani@aut.ac.ir
1021-9986/2021/4/1411-1435 22/$/7.02

Iran is forced to produce valuable oil gas and petrochemical derivatives. It is more than fossil fuels and has greater economic benefits for the country, investing specifically to create scientific enterprises and use more renewable fuel technology to prevent environmental pollution. One of the most important problems in Iran is the waste of fluorine gases, by examining different recovery methods, can find and implement a suitable method according to climatic conditions, etc. conversion of gas to liquid is one of the ways to create added value and recovery of fluorinated gases, which over the past two decades, many countries have tried to create technology and operate these systems. The gases sent to the flares cause a lot of pollution for various reasons, including incomplete combustion, but these gases also have a high fuel value. The following three items illustrate the importance of research on this topic. Annually, over 150 billion cubic meters of gas in the world are converted into pollutants under the name of flare (or burning of gases by a burner), which represents a waste of 15 to 20 billion dollars, which according to the World Bank, is equivalent to one-third of gas consumption in the whole of Europe, or residential gas consumption in America[1]. About two-thirds of the Persian Gulf flare is related to Iran, while two decades ago, it was different, and Saudi Arabia was known as the owner of the largest flare in the region. Which has been used to prevent flaring by launching a gas pipeline network in the domestic market [2]. South Pars gas field (with North Dome's name on Qatar) is the largest independent gas field globally, located jointly between Iran and Qatar. This common field has about 40 trillion cubic meters of gas, accounting for more than 21% of the world's total gas. The area of this square is 9700 square kilometers, of which 3700 square kilometers belong to Iran. Gas reserves of this part of the gas field for Iran's share are equivalent to 14.2 trillion cubic meters with 19 billion barrels of gas condensate, including about 8% of the world's total gas and about 47% of the country's gas reserves [3]. Liquefied Natural Gas (LNG) processes need high power to produce the LNG [1]. Various process configurations have been proposed to reduce the required refrigeration. Specific Energy Consumption (SPE) or liquefaction efficiency is a parameter that is used to evaluate the LNG process energy consumption. This parameter is defined as the required power to produce one kilogram of LNG (kW/kg LNG) [1]. Commercial refrigeration systems in LNG processes are classified based on the configuration and working fluid [2]. Refrigeration systems are classified into three sections: Single-stage, cascade, and multistage. Energy consumption in nitrogen single and dual expander processes of natural gas liquefaction is investigated. A three-stage propane cycle of the cascade LNG process is analyzed by the exergy method [3]. Mixed refrigerant composition is optimized in a Single Mixed Refrigerant (SMR) process [4]. This study proposes a new method for finding the mixed refrigerant composition based on exergy efficiency minimization. Optimization of mixed refrigerant systems in low-temperature applications is investigated by a Group Method of Data Handling (GMDH) [5]. A novel LNG process that uses two MR cycles is proposed and analyzed [6]. Integration of the natural gas liquefaction process with a process that operates at cryogenic temperatures is an effective idea that can decrease the required refrigeration in both of them. Hydrocarbon recovery processes are one suitable candidate for integration. This idea has been investigated in several papers [2,7,8]. A propane refrigeration cycle provides the required refrigeration in the Natural Gas Liquids (NGL) recovery process [9–12]. The process outputs are NGL and residue gas. A distillation column, a demethanizer column, is used for reaching the desired ethane recovery. Residue gas is injected into the pipeline gas for transmission and distribution [10–17]. Decreasing the required refrigeration against the ethane recovery level is considered to optimize the hydrocarbon recovery processes [15]. The combined pinch and exergy Efficiency of an NGL recovery process is improved by applying the exergy analysis [18]. Two regasification processes for NGL recovery from LNG are investigated [19]. The results show that the low-pressure process is more economical than the high-pressure process because saving in TAC is higher by 4.6%. A novel small-scale integrated mixed refrigerant (MR) LNG plant and NGL recovery process is proposed and optimized [8]. This process can produce LNG and NGL with low energy consumption. In this study Genetic Algorithm (GA) is used for optimization. Natural gas liquids (NGL) containing ethane and heavier hydrocarbons are separated from the feed gas for added value. A novel absorption process is introduced for dew point control of natural gas streams [20]. A new concept called: Novel LNG-Based integrated process configuration alternatives

are introduced [2]. This study converts three conventional LNG processes (MFC, DMR, C3MR) to integrated NGL-LNG processes. Ethane recovery and specific powers are 90% and 0.4 kWh/kg-LNG, respectively. A novel integrated process that uses mixed refrigerant cycles is proposed for the production of NGL and LNG. The liquefaction efficiency in this process is 0.414 kWh/kg LNG. Also, it can recover ethane higher than 93.3% [7]. Decreasing the required power in the refrigeration systems is why a combination of these two processes is investigated. Energy and exergy analysis methods are used to evaluate the cryogenic natural gas processes [21,22] Exergy-pinch analysis is used to optimize the refrigeration cycle in NGL recovery plants [9]. Small-scale Liquefied Natural Gas (LNG) liquefaction processes, SMR, two-stage expander nitrogen refrigerant, and two open-loop expander processes are investigated using the exergy analysis method [23]. Based on the modified Claude cycle, large-scale helium liquefaction systems with two expanders are discussed and analyzed [24]. In this study, exergy analysis is applied to consider the behavior of the helium liquefaction process. A double-effect absorption refrigeration system is investigated, and a comparative analysis is performed based on the exergy destruction [25]. A novel NGL recovery process is introduced and analyzed [26]. In this study, ethane and propane plus recoveries are greater than 90% and 95%, respectively. A combined cogeneration system with steam and gas turbines is investigated by energy efficiency analysis [27]. A performance analysis is done on a reversible Otto cycle [28]. Irreversible cogeneration systems are optimized under alternative performance criteria [29]. Efficiency analysis of the irreversible Brayton cycle is investigated based on alternative criteria [30]. Finite-time thermodynamic analysis of an internal combustion dual cycle is considered [31]. However, exergy analysis can reveal the process components' irreversibility and exergy efficiency, but improving the system performance based on the exergy analysis results is not always profitable based on economic analysis. To consider the economic principles in the design and analysis of energy-intensive processes, thermoeconomic analysis is a more useful tool. Exergoeconomic diagnosis of the SMR process, Linde and Air Products and Chemicals Inc, are investigated [32,33]. In these papers cost of investment and exergy destruction of the components are calculated. Multistage mixed refrigerant liquefaction processes are identified by the advanced exergoeconomic analyses method [34]. An industrial propane refrigeration cycle used in the NGL recovery process is investigated using thermoeconomic analysis [10]. In this study, intrinsic and induced malfunctions of the components are analyzed and quantified. The Organic Rankine Cycle (ORC) performance in three different process configurations is analyzed by thermodynamic and exergoeconomic models [35]. The results show thermodynamic and economic analysis methods propose different processes with optimal performance. An integrated biomass gasification and gas turbine power plant is analyzed by comparative exergoeconomic analyses [36]. Relative cost difference and exergoeconomic factors are calculated for the proposed system in this study. Exergetic, exergoeconomic, and exergoenvironmental analyses are applied to the Fischer-Tropsch unit liquefaction process [37]. Another study evaluates the main flare gas recovery alternatives, including sweet gas production, Gas to Liquid (GTL), and power generation, by using exergy and exergoeconomic analysis tools. For this purpose, flare gas condition in two phases of the Pars Special Economic Energy Zone in the south of Iran was chosen as a case study[38]. A related study also considered the feasibility of three methods for FGR, which is evaluated in a giant gas refinery in Iran. The first two methods considered liquefaction and LPG production by implementing flare gases as feed for the existing LPG unit. Different parameters were studied in feed liquefaction and LPG production. The third studied option is using a three-stage compression unit to compress the flare gases. Finally, an economic evaluation was performed to find the most profitable method[39]. Also, another novel NGL/LNG integrated scheme based on the C3MR refrigeration system is modeled using Aspen plus® in this study. The mentioned scheme utilizes mixed refrigerant to provide some of the required cooling in the ethane recovery unit and produce LNG with the low power consumption studied in the ref. [40]. The optimal operating conditions for the proposed configuration are determined by considering the earned profit. A surrogate model is formulated by exploring the design space based on the response surface methodology. The optimal conditions from the mathematical model are obtained using a genetic algorithm. Finally, a paper presents a complete and concise PI framework, which depends

on rated energy consumption as a key driver for implementation, where the rating implicitly considers multiple other criteria. The framework also classifies the potential PI tools for the O&G into separation and reaction tools, while the PI traditional hierarchy classifies them into equipment and methods. The process-based classification reflects better the specifics of O&G and facilitates proper tool selection by designers. According to this framework, the paper examines the potential of important technologies found in the literature. Drivers and constraints concepts are considered, and a map of the PI implementation in the main O&G facilities is provided [41].

Iran is known as the third country to burn flare gas in the world. As a result of research on the recovery of flare gases, etc., it can improve the environment, and economy and create added value in the country. In this paper, the recovery method through the liquid fuel production system from flare gas has been investigated due to this issue's importance. Exergy efficiency and exergy destruction of the process components are calculated. Next, all equipment is sized, and the cost is calculated with a suitable cost function. Mathematical modeling of the process is done to find the exergoeconomic factors. Next exergoeconomic variables, exergy destruction cost, relative cost difference, exergoeconomic factor, are computed, and thermoeconomic analysis of the process is investigated and discussed.

THEORETICAL SECTION

Several methods have been proposed to recover flare gas so far the use of FGRS system [7] is one of the efficient methods in this group, which has also been used, of course, to find a suitable solution to use flare gas according to the type The refinery, petrochemical, etc. industries need to be examined in different ways. These include collecting flare gas and injecting it into oil wells, collecting and storing it in underground reservoirs, producing hot water or steam using the heat of burning gas, producing liquefied petroleum gas from gas, increasing pressure, generating electricity, and so on. The final diagnosis depends heavily on several factors, including location geography, and economic evaluation, for example, refinery gas recycling uses deep cooling, and deep cooling technology to separate hydrocarbons, nitrogen, hydrogen, heavy water, and helium. Gives. Calculations and analysis for one of the Moscow refineries with about 65,000 cubic meters of exhaust gas per hour show that if the deep cold is used, the equivalent of 4,000 kg of ethylene, 3,500 kg of propylene, 15,000 kg of a heavy hydrocarbon mixture, up to 10,000 kg of propylene can be used per hour. , Produced 3,500 kg of nitrogen, and eventually up to 3,000 kg of hydrogen [4]. Due to the low price of natural gas and to earn more money, over the years, the technology of producing liquefied petroleum gas from gas and the improvement of leading companies in this industry, and the cooperation of their governments caused them to approach the most acceptable point economically. From 1950 to 1990, SASOL operated in South Africa to convert coal to hydrocarbons using the Fisher-Trap process annually in three industrial units with a total capacity of 4,000,000 tons per year. There are currently two active industrial units and several projects around the world. Sell has also been active in the city of Bento, Malaysia, since 1980, using the Fisher-natural gas-to-fuel process and other products. Other countries, such as Qatar and Nigeria, use this system [5]. Hence, this method has also been evaluated as a way to convert fluorine gas to liquid fuel. An example of this evaluation is Parsian Refinery, which has used liquid fuel production technology from Flare gas, with an evaluation output of 563 barrels of GTL products per day [6] Assaluyeh region according to the information collected. Before 2012, it was equivalent to 48056 barrels of GTL products per day [7].

CDM clean development mechanism

It is a plan by which developed and committed countries to implement the Kyoto Protocol to reduce greenhouse gas emissions, and Developing countries also reduce emissions in return. Or receive CER [9] as a sum of money. Because it is generally possible to prevent and reduce greenhouse gas emissions in developing countries at a lower cost than in developed countries, many developed countries are interested in implementing this plan in developing countries. As a result, a developed country invests in a developing country, which leads to technology transfer, job creation, improving environmental conditions, etc., in a developing country. In addition to the above, revenue is also generated before the emission reduction certificate and reduced fuel costs and consumables of the developing country [8]. CDM projects in the country are divided into three groups: registered, under review by operational institutions, and the preliminary stage

(initial announcement). Some of these cases are Jahrom Combined Cycle Power Plant, Piran Hydroelectric Power Plant, the collection of associated gases in Nowruz and Soroush fields, the replacement of natural gas instead of fuel oil in Amirkabir sugarcane industry, replacement of natural gas instead of fuel oil in Dabal Khazaei sugarcane industry [9].

Flare gas (torch)

The word torch is used to describe an unopened (open) flame that burns excess gases. This process occurs in upstream oil and gas facilities, oil and gas refineries, and petrochemical and mining industries. Burners emit large amounts of gas into the air in a short time. The amount of gas burning in the burner depends on its efficiency, combustion process time, etc., which is usually due to the lack of sufficient time for combustion and improper efficiency of the burners; some unburned gas enters the atmosphere. According to 2,000 official papers published in Canada, 250 different known toxic substances are released into the air during the combustion process, significantly affecting the environment [10]. Gas metering equipment in the Flare system The most important factor in monitoring and controlling the Flare system is the gas flow meter and gas flow analysis. In some countries, such as Norway, all Flare systems are equipped with flow meters or standard meters, which have been developed to measure flare gas flow. The value of fluorinated gases determines the revenue from the sale of recycled gases, which is important in the whole project's economic review. For example, a burner with a diameter of 30 inches, if the flame height is 30 feet, the heat and expense value of the gases sent to the flare would be 100 million BTU per hour and $1,752,000 per year [11-27].

History of gas-to-liquid conversion GTL

Fischer-Tropsch synthesis developed in the 1920s, when the German steel industry looked to make the best synthetic gas from coke steel. At this time, reactions such as the amber synthesis by the Haber method also spread. Before Fischer and Tropps succeeded in synthesizing heavy hydrocarbons from synthesized gas, in 1913, the German scientist Friedrich Bergius Invented a catalytic process for extracting hydrocarbon liquids from coal in the presence of hydrogen. In parallel with Bergius' research, in the 1920s, two other German scientists, François Fischer and Hanstropesch were looking to produce hydrocarbon fuels from coal-based gas. In the method developed by these two, coal molecules were synthesized into gas under underwater vapor pressure and converted into heavier hydrocarbons with suitable catalysts. Coal synthesis gas was converted to heavier hydrocarbons with suitable catalysts [27-38]. The GTL process converts gas fuel to liquefied fuel, which has recently attracted much attention due to its many benefits, especially through the Fisher-trap synthesis process, which has a very low sulfur content. And preserves aromatic compounds. GTL emits few pollutants and is considered a clean (green) fuel [13]. The GTL system consists of three parts of gas purification (removal of H_2S and CO_2), synthesis gas production, FT-process (production of hydrocarbons), upgrading, and improving product quality is considered the fourth part. The main advantages of the GTL process are the low density of GTL products, no aromatic compounds in products, the very low and insignificant concentration of sulfur in the product, the higher cetane number of obtained products, creating higher added value than natural gas and the possibility of using gases that are sent to flare for burning in refineries [39-70].

South Pars gas field

South Pars gas field is one of the main energy sources in the country(see Fig. 1). The South Pars gas field's development aims to meet the growing demand for natural gas, inject oil fields, export gas, gas condensate, and supply feed to petrochemical complexes. This huge field development plan has been planned in 24 phases so far [3]. Flare in South Pars refineries can be summarized in 4 types, which include High-Pressure (HP) burners, Medium-Pressure (MP) burners, Low-Pressure (LP), burners, and torches related to storage units of propane and butane (LPG) [70-92].

Research methods

To enter the main part of the research topic and achieve an acceptable numerical output in an industrial unit, it is necessary to simulate that unit with software. Therefore, the GTL unit has been simulated using Aspen Hysys software, but the two main points to be implemented are Flare gas analysis and its operating conditions, which will be mentioned below. According to the software used, the most important factor in the simulation of units has

Table 1: Flare gas analysis of sample refinery (design values).

Composition	LP-Flare	MP-Flare	HP- Flare
Methane	88.18	88.28	85.55
Ethane	4.52	4.83	5.19
Propane	1.61	1.70	2.07
i-Butane	0.31	0.32	0.46
n-Butane	0.47	0.49	0.78
i-Pentane	0.00	0.04	0.07
n-Pentane	0.00	0.03	0.05
$C6^+$	0.05	0.05	0.45
CO_2	1.27	1.04	1.51
N_2	3.57	2.86	3.87

Fig. 1: Map of South Pars gas field.

the input feed analysis to transfer to the desired unit that we want to do the simulation that must be examined. The sample refinery (the third refinery - phases 4 and 5 of South Pars) has an H_2S level of 1000 ppm. At this point, it is assumed that: $C6^+$=C7 (see Table 1).

The second assumption is that the flow rates and the specifications listed in table 2 are constant; according to this information, simulators related to each part have been performed[92-101].

Liquid fuel production unit (GTL) simulation

In the first stage (purification), first, the set of flare gases is brought to the same pressure, and after passing through the two-phase separator (D-100-1), it is sent to the compressor to reach a pressure of 68 bar again from a two-phase separator. (D-100-2) Pass and then be absorbed by the tower. These towers are composed of several trays placed at specific distances to create Contact between the two phases of gas and liquid. The important point in this part is to use the type of amine, the liquid phase (amine) enters from the top of the absorption tower, and the gas phase enters from the bottom of the tower and due to the force of gravity and the Contact of the two phases and the law of mass transfer, sour gas by solution The amine is separated and the sweet gas moves to the top of the tower[101-107]. Several trays + amine solution purifies sour gas.

Table 2: Operational analysis of flare gas of sample refinery (design values).

Description	Temperature	Pressure	Volumetric Flow Rate
HP-Flare	25°C	5.01 bar	6MMSCFD
MP-Flare	25°C	1.71 bar	6MMSCFD
LP-Flare	25°C	1.05 bar	6MMSCFD

The number of trays in this tower is 20, and the pressure difference from top to bottom is 0.2 bar.

In this simulation, the second type of amine, namely [12] DEA, is used. Increasing the concentration of diethanolamine causes the uptake of acid gases. The separator becomes biphasic. At this stage, light hydrocarbons are separated from the separated amine. The enriched amine enters the heat exchanger (H-EX) [13] with the repulsion tower's Lean Amine solution. The heat exchange data is added to its temperature and enters. The tower is repelled. The regeneration tower is the opposite of the absorption tower, i.e., the temperature is high, and the pressure is low. As a result, more acidic gases are separated from the amine in the regeneration tower. The high temperature is created by the reboiler at the bottom of the regeneration tower and causes evaporation. Acidic gases evaporate as a vapor phase and pass upstream of the discharge tower - enter the condenser and exchange heat. Two phases of vapor and liquid are formed, the liquid part returns to the discharge tower, and the vapor of the acid gases is released - They are removed manually and enter the heat exchanger, which loses some of its temperature for the enriched amine, and with the Makeup, H_2O enters the heat exchanger (E-103) to reduce the temperature, then by the pump (P-100). The pressure increases and returns to the top of the absorption tower. In this part of the simulation, the amount of sweetened gas equal to MMSCFD [14] is 17.72, with a pressure of 68 bar and a temperature of 35 degrees. H_2S isolated in the sweetening unit can also be directed to sulfur recycling units (see Fig. 2).

The mixture of hydrogen and carbon monoxide with different ratios between the two is referred to as the general synthesis gas; given that the total output of the flares (molar flow rate) is lower than the natural gas used in these systems, oxygen production is expensive. Steam reforming is used in the synthesis gas production system, and three reactors are used; one conversion reactor and two equilibrium reactors (as a pre-reforming unit and a reforming unit) are used for simulation. The sweetened gas enters the heat exchanger (E-100) to be prepared for pre-reforming operations. The required water (steam) (taken from other units, etc.) enters the pre-reforming, according to the temperature range in the reactor, Which is also of the conversion type between 350-550°C (12) should be considered here 500 °C and pressure range between 20-40 bar [16-17] which is selected 25 times, this pressure is Fisher trap is maintained until the last stage, at which point heavy hydrocarbons are converted to methane. The following reactions are the reactions used in pre-reforming:

$$C_5H_{12} + 4H_2 \rightarrow 5CH_4 \quad (1)$$

$$C_4H_{10} + 3H_2 \rightarrow 4CH_4 \quad (2)$$

$$C_3H_8 + 2H_2 \rightarrow 3CH_4 \quad (3)$$

$$C_5H_6 + H_2 \rightarrow 2CH_4 \quad (4)$$

$$C_7H_{16} + 6H_2 \rightarrow 7CH_4 \quad (5)$$

The reactions that occur in the reforming process are as follows:

$$CO + 3H_2 \leftrightarrow CH_4 + H_2O \quad (6)$$

$$\Delta H_{298K} = +206 \frac{kJ}{mol}$$

$$CO + H_2O \leftrightarrow O_2 + H_2 \quad (7)$$

$$\Delta H_{298K} = -41 \frac{kJ}{mol}$$

Considering the oxidation of natural gas, which is an endothermic process, applying heat flow following the process and adjusting the output current's temperature increases the synthesis of output gas. The produced gases enter the equilibrium reactor (Shift-Reformer) with the mentioned conditions. By selecting (bad source), the Gibbs free energy of the reaction is done, the output temperature reaches about 700°C, and the output of the equilibrium reactor passes through a heat exchanger to the temperature.

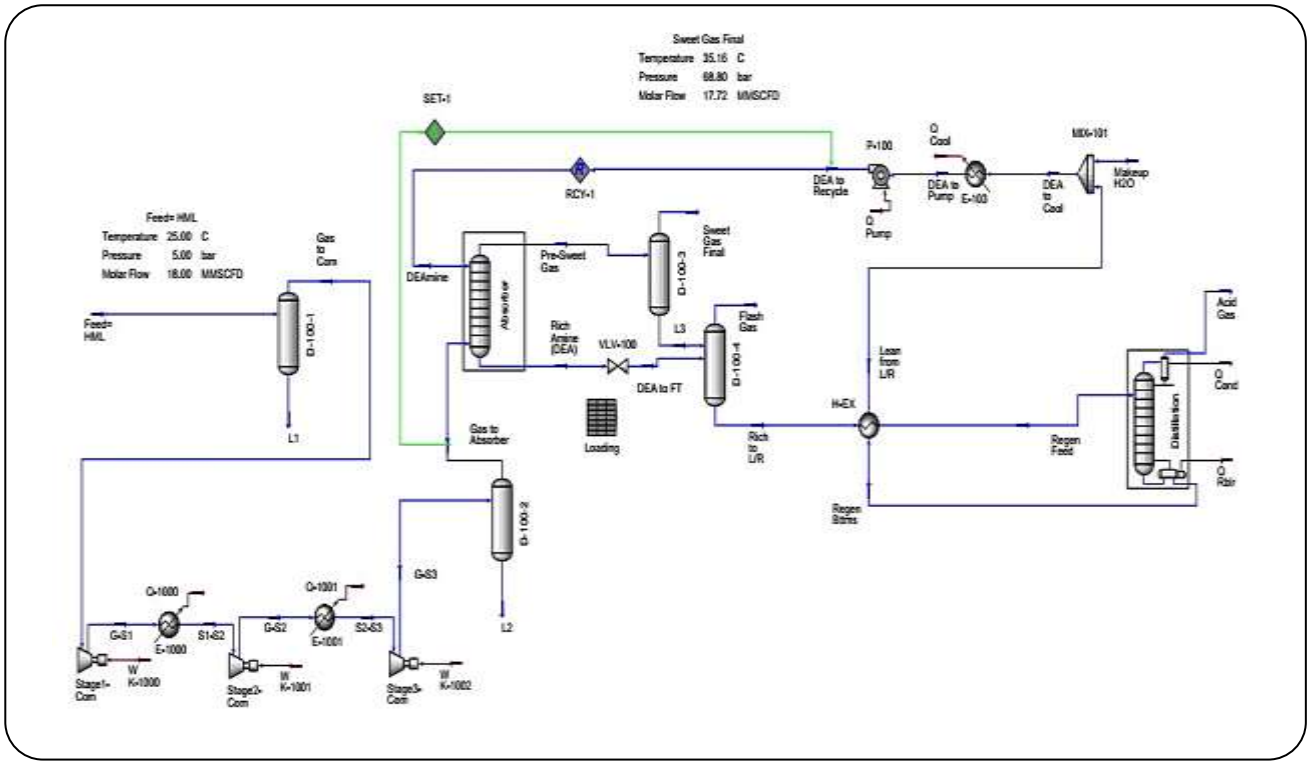

Fig. 2: Schematic simulation of sweetening unit.

It reaches about 1000 ° C with a constant pressure of 25 times, this output enters the second equilibrium reactor, which simultaneously enters the superheated equilibrium reactor with a temperature of 500 °C, the reforming output temperature is between 700 to 900 °C (16) and usually 900 °C has been selected. Also, the need for CO_2 to react to obtain a suitable synthesis gas is necessary to enter the Fisher-Trap process and produce more products, considering that the H_2:CO ratio is 1.8, using a Cobalt catalyst. CO_2 is calculated using Spreadsheet, the amount of CO_2 equals 14.48 MMSCFD, and finally, the synthesis gas - the major percentage of which includes hydrogen and carbon monoxide - synthesis gas with a temperature profile of 900°C, 25 bar, and 86.63 million ft^3/day to the Fisher trap reactor in Fig. 3 is a synthetic gas unit simulation.

Fischer - Tropsch process simulation

Considering that the Fischer therapy process is exothermic, the lower the conversion temperature, the higher the final conversion rate, but this also depends on the type of catalyst and, of course, the design conditions (limitations such as environmental, technical, and economic conditions). Before the feed enters the reactor, it first enters a cooler (E-102) to reduce its temperature and then prepares to enter the Fisher Trap reactor. Depending on the type of product and conditions, the temperature range of Fisher Trap can be high temperature (HTFT) or low temperature (LTFT), i.e., 320-340 ° C and 220-240 °C, respectively (12), which is high temperature with the choice of iron catalyst for gasoline production and low temperature is considered using cobalt catalyst for waxy production, in which 220 °C temperature and cobalt catalyst type are selected. The type of reactor used in this stage is the tubular shell reactor. They were chosen because they are easier to maintain due to the lack of moving parts, and the high conversion percentage for this part has been selected. Fisher-Trap Reactor Defines all possible reactions. By entering the C1-C30 reactions in Hysys software and the operating conditions, these depend on the type of catalyst and the Anderson-Schulz-Fluorine (ASF) distribution or vice versa. The probability factor of hydrocarbon chain growth is selected $\alpha = 0.8$ and considered for $W_n = n(1-\alpha)^2\alpha^{n-1}$. The FT reactor's output is now sent to a coolant (E-103) and then sent to a three-phase separator (V-100) to separate light, heavy, and water compounds. Fig. 4 shows a simulation of the Fisher-Trap process unit.

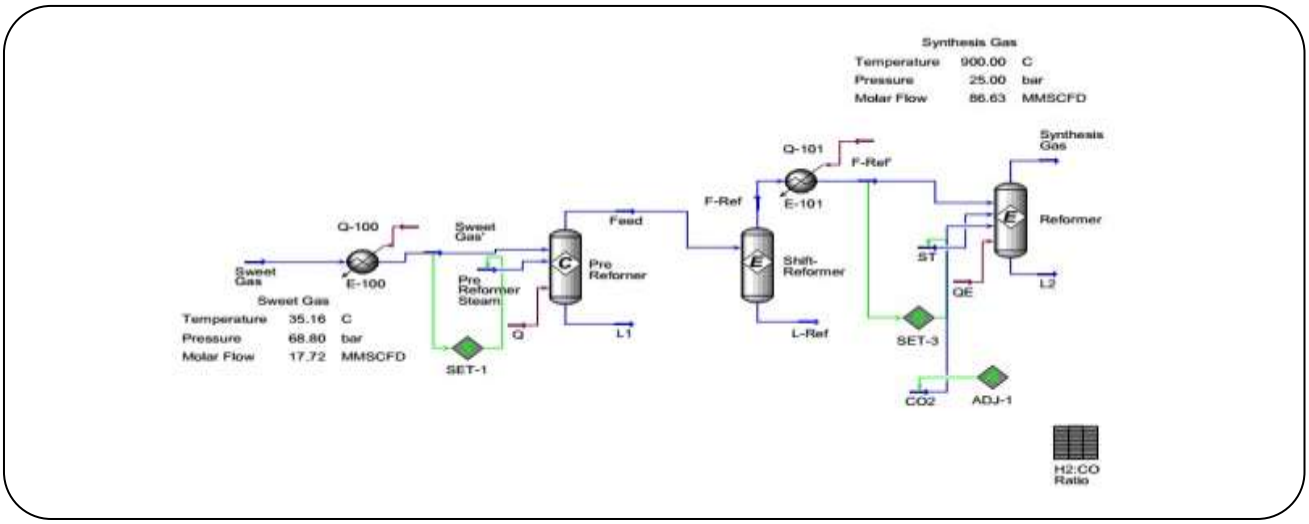

Fig. 3: Simulation schematic of synthesis gas unit.

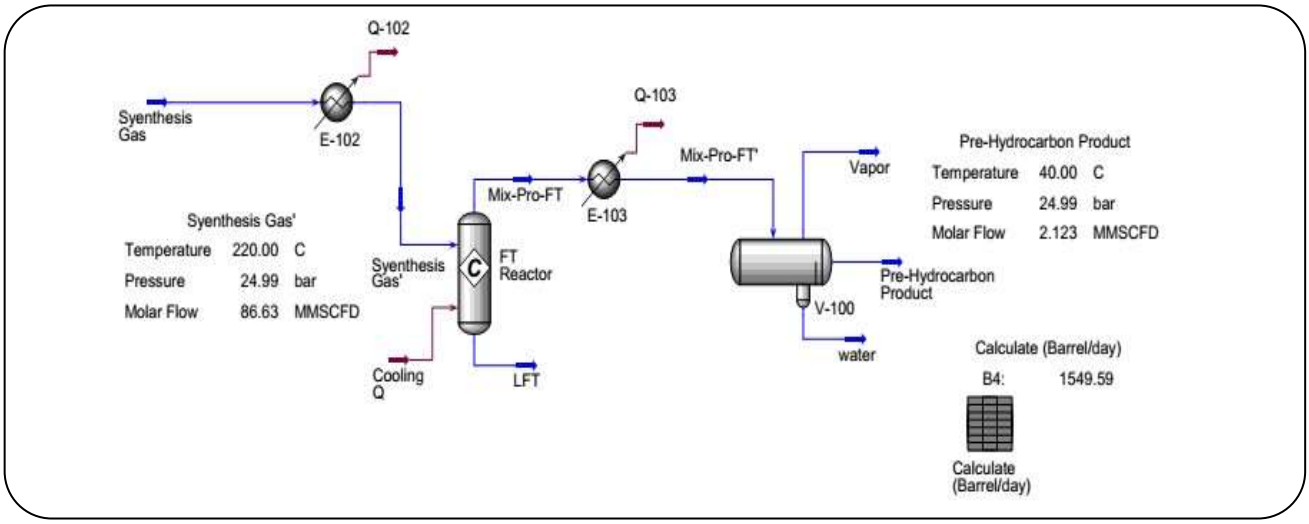

Fig. 4: Schematic of Fisher Trap process unit simulation.

Exergy and Exergoeconomic analysis

Energy is found in different forms (electrical energy, mechanical energy, and thermal energy) that can be converted with limitations (see the first law of thermodynamics). When converted to another type, some types of energy can only be considered by considering the environmental conditions and the qualitative impact on the environment, meaning the second law of thermodynamics in thermodynamic systems. As a result, it can be said that different forms of energy have variable quantities and qualities. Exergy knowledge helps us to define these changes well and to monitor the optimization of energy balance. Electrical and mechanical energy can be called gross exergy, while thermal energy is wasted in converting it to other energy types. Exergy is a type of energy modeling based on the first and second laws of thermodynamics. Analytical application of exergy helps us to find the amount of energy wastage in processes that reach equilibrium.

Advanced exergy analysis is based on the results of exergy analysis. In this analysis, equipment's irreversibility is divided into two perspectives: the origin of irreversibility, and the other irreversible. From the first point of view, any device's irreversibility is divided into endogenous irreversibility and exogenous irreversibility. Endogenous irreversibility is the part of irreversibility that relates to the inherent function of the device. Exogenous irreversibility is part of the irreversibility that is the induced effect

of irreversibility in other devices. Therefore, in this view, the destructive exergy other than k can be shown as follows:

$$E_{D,k} = E_{D,k}^{EN} + E_{D,k}^{Ex} \quad (8)$$

There are two methods for calculating endogenous destructive energy. The thermodynamic and engineering methods discussed in this paper from the engineering method of exaggerating the hybrid should be discussed in detail (see Fig. 6).

$$E_{D,tot} = E_{F,tot}^{\cdot} + E_{P,tot}^{\cdot} \quad (9)$$

$$E_{D,tot} = \sum_{k} E_{D,k}^{\cdot} = E_{D,k}^{\cdot} + E_{D,ther}^{\cdot} \quad (10)$$

Exogenous destructive exergy can be obtained by calculating endogenous destructive exergy and using the following relation.

$$E_{D,k}^{EX} = E_{D,k}^{\cdot} - E_{D,k}^{EN} \quad (11)$$

From the point of view of the ability to eliminate irreversibility, each device's irreversibility is divided into two parts: avoidable irreversibility and unavoidable irreversibility. Inevitable irreversibility ($E_{D,k}^{UN}$) is a part of irreversibility that cannot be eliminated. The criterion of whether or not irreversibility can be eliminated is technical and economic limitations in the design, construction, or selection of devices. From this point of view, the amount of destructive exertion can be written as follows:

$$E_{D,k}^{\cdot} = E_{D,k}^{UN} + E_{D,k}^{AV} \quad (12)$$

In this paper, the assumptions for determining the inevitable irreversibility, as shown in Table 2, are considered.

Destructive exergy values are unavoidable and avoidable from the following equations:

$$E_{D,k}^{UN} = E_{P,k}^{\cdot} \left(\frac{E_{D,k}^{\cdot}}{E_{P,k}^{\cdot}} \right)^{UN} \quad (13)$$

$$E_{D,k}^{AV} = E_{D,k}^{\cdot} - E_{D,k}^{UN} \quad (14)$$

Then, to better understand each component's role in the process, these irreversibilities can be combined. As a result, four sets of irreversible endogenous irreversible, exogenous unavoidable, endogenous avoidable, and

Table 2: Advanced exergeo-economic analysis hypotheses.

Component	Operational state
Compressor	90%
Heat exchanger	$\Delta T_{min} = 0.5C$
Air Cooler	$\Delta T_{min} = 5C$

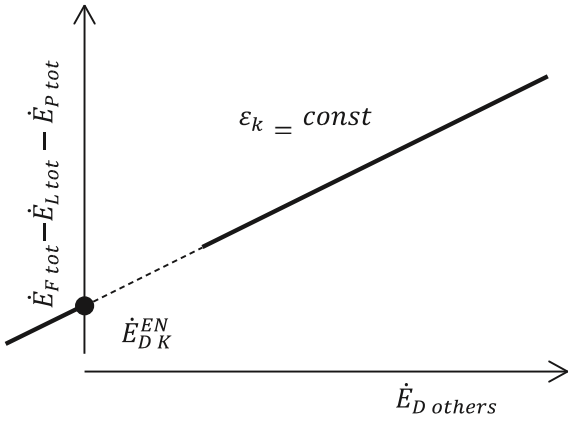

Fig. 6: Schematic of the engineering method for calculating endogenous destructive exergy. When drawing this diagram, the energy performance should remain constant except for the k th component.

exogenous avoidable are created. The various unavoidable endogenous and exogenous irreversible types of equipment are defined as follows:

$$E_{D,k}^{UN,EN} = E_{P,k}^{EN\cdot} \left(\frac{E_{D,k}^{\cdot}}{E_{P,k}^{\cdot}} \right)^{UN} \quad (15)$$

$$E_{D,k}^{UN,EX} = E_{D,k}^{EN\cdot} - E_{D,k}^{UN,EN} \quad (16)$$

The various avoidable endogenous and exogenous irreversible types of equipment are defined as follows:

$$E_{D,k}^{AV,EN} = E_{P,k}^{EN\cdot} - E_{D,k}^{UN,EN} \quad (17)$$

$$E_{D,k}^{AV,EX} = E_{D,k}^{AV\cdot} - E_{D,k}^{AV,EN} \quad (18)$$

Exergoeconomic analysis is a combination of exergy analysis and economic analysis. The purpose of this analysis is to obtain the exergy cost of each flow. In general, this equation is written as follows:

$$c_{F,k} E_{F,k} + Z = c_{P,k} E_{P,k} \quad (19)$$

Auxiliary equations are also required for components with more than one output current. Therefore, by writing the above relations for all the components of the process and the auxiliary relations, a system of linear equations is obtained, including the unknowns of each flow's unit cost. By solving this device, in addition to these unknowns, the exergy cost of each currency can be calculated through the following equation.

$$C = cE \tag{20}$$

$$C_{D,k} = c_{F,k} E_{D,k} \tag{21}$$

As in advanced exergy analysis, in advanced exo-economic analysis, the cost of destructive exergy and each component's investment cost is divided into endogenous/exogenous and non-avoidable / avoidable. The following equations can obtain endogenous, exogenous, unavoidable, and avoidable destructive exergy cost values.

$$C_{D,k}^{EN} = c_{F,k} E_{D,k}^{EN} \tag{22}$$

$$C_{D,k}^{EX} = c_{F,k} E_{D,k}^{EX} \tag{23}$$

$$C_{D,k}^{UN} = c_{F,k} E_{D,k}^{UN} \tag{24}$$

$$C_{D,k}^{AV} = c_{F,k} E_{D,k}^{AV} \tag{25}$$

$$C_{D,k}^{UN,EN} = c_{F,k} E_{D,k}^{UN,EN} \tag{26}$$

$$C_{D,k}^{UN,EX} = c_{F,k} E_{D,k}^{UN,EX} \tag{27}$$

$$C_{D,k}^{AV,EN} = c_{F,k} E_{D,k}^{AV,EN} \tag{28}$$

$$C_{D,k}^{AV,EX} = c_{F,k} E_{D,k}^{AV,EX} \tag{29}$$

Costs of investment can be calculated from the following equations.

$$Z_k^{EN} = E_{P,k}^{EN} \left(\frac{Z}{Ep} \right)^{real} \tag{30}$$

$$Z_k^{EX} = Z_k - Z_k^{EN} \tag{31}$$

$$Z_k^{UN} = E_{P,k}^{\cdot} \left(\frac{Z}{E_p} \right)^{UN} \tag{32}$$

$$Z_k^{AV} = Z_k - Z_k^{UN} \tag{33}$$

$$Z_k^{UN,EN} = E_{P,k}^{EN} \left(\frac{Z}{E_p} \right)^{UN} \tag{34}$$

$$Z_k^{UN,EX} = Z_k^{UN} - Z_k^{UN,EN} \tag{35}$$

$$Z_k^{AV,EX} = Z_k^{UN} - Z_k^{UN,EN} \tag{36}$$

$$Z_k^{AV,EX} = Z_k^{EX} - Z_k^{UN,EX} \tag{37}$$

RESULTS AND DISCUSSION

Exergy analysis

Fig. 7 shows the Process Flow Diagram (PFD) of the MFC is shown. As we have seen, the recovery of natural gas liquids and LNG production is done in an integrated process [22]. A brief description is provided, and for more details, you can refer to the available reference. For accurate and easy analysis, the use of the software is inevitable. Therefore, for this project, Aspen Hysys V11 software has been used to simulate operational units.

First, we present the table of thermodynamic information related to currents. Information on comparing the percentage composition of each component of the actual input current and comparing it with its simulated sample is presented in Table 3.

Tables 4 and 5 show the results of performing exergy calculations on the main process units of the Etana recovery unit. Since there is no possibility of calculations in a single method in some units, the flow method's calculations related to these process units have been done.

Figs. 8-10 show the exergy destruction rate and share and exergy efficiency of each component. The results illustrated in these figures show the most exergy is destructed, thus the greatest potential for a retrofit in the process.

According to the arrangement in Fig. 7, the system is designed. In Fig. 13, the total destructive exergy diagram for different process types is drawn for different process equipment, except for the desired equipment. As can be seen, there is a linear relationship between these two parameters. The width from this sample's origin is equipped with an endogenous dissipation exergy indicator for each component. The 104-E-101 converter with 5900.9 kW, the 105-E-101 compressors with 3863.7 kW, and the 105-E-106 with 3099.3 kW have the most endogenous destructive energy. Also, 105-X-101 air coolers with 32.013 kW, 105-K-101 with 69.929 kW, and 111-K-101/2 with 94.111 kW have the least endogenous destructive exergy.

Table 3: Simulation Results of the PFD system.

Stream	Pressure (bar)	Temperature (C)	Molar flow (kmol/h)	Stream	Pressure (bar)	Temperature (C)	Molar flow (kmol/h)
51	61.60	28.10	23650.10	145	4.11	4.50	450.00
52	60.60	35.10	23650.10	146	4.01	2.65	450.50
53	60.60	35.10	1035.50	149	22.65	78.85	4306.30
54	30.50	66.40	15914.70	217	30.25	33.60	2688.25
55	30.30	48.30	1035.40	218	30.22	43.80	952.15
56	29.40	17.00	21,915.00	219	30.94	99.00	3288.80
57	28.70	33.75	21915.10	220	30.95	109.30	2431.00
58	30.30	43.80	1736.10	228	50.05	2.90	1003.80
59	30.90	43.80	1736.10	244	60.55	35.00	22614.70
60	30.60	10.70	2683.00	247	60.35	85.00	6700.00
61	30.10	9.20	1804.80	248	30.05	87.90	21,914.00
62	33.70	49.20	21915.10	249	30.10	8.20	2677.00
63	30.10	9.20	878.30	250	30.10	43.70	3067.00
64	31.00	109.30	857.80	256	30.05	16.00	2677.00
142	82.10	19.00	3692.60	257	81.05	20.70	610.70
143	82.10	19.00	610.70	261	30.00	16.50	3067.00
144	51.10	2.50	1003.70	D-12	65.05	47.00	475,586

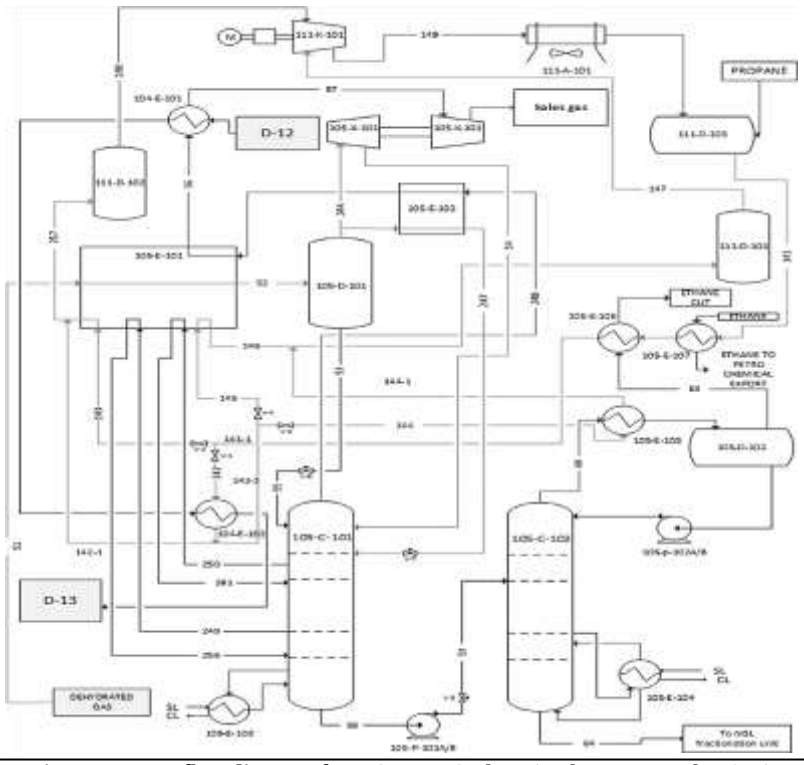

Fig. 7: Process flow diagram for NGL+LNG plant (Mehrpooya et al., 2014).

Table 4: Exergy Analysis Results of the PFD system.

Stream	Physical exergy (kW)	Chemical exergy (kW)	Total exergy (kW)	Stream	Physical exergy (kW)	Chemical exergy (kW)	Total exergy (kW)
51	61479.25	5671500	5732965	145	590.96	258115	258704
52	64021.45	5671500	5735530	146	402.06	258115	258523.5
53	2375.57	475000	477375	149	8060.37	2461925	2469905
54	38813.2	3658450	3697305	217	4574.63	1365910	1370470
55	2248.65	475000	477251.5	218	1925.65	422997	424925.5
56	47573.15	4732425	4780020	219	4529.89	2141490	2145955
57	47247.3	4732425	4779640	220	4944.28	1545555	1550495
58	2709.59	942960.5	945668	228	1020.59	574788	575814
59	2712.25	942960.5	945677.5	244	61028.95	5198685	5259675
60	5562.44	1066565	1072075	247	22915.9	1540045	1562940
61	3923.22	719558.5	723415.5	248	55671.9	4731950	4787620
62	49654.6	4732425	4782110	249	4925.56	1295990	1300930
63	1839.11	347700	349524	250	7139.25	1324300	1331425
64	1106.75	596020.5	597122.5	256	4875.12	1295990	1300930
142	4932.31	2111090	2116030	257	780.82	349134.5	349913.5
143	815.42	349134.5	349951.5	261	6437.96	1324300	1330760
144	1336.27	574788	576127.5	-	-	-	-

Table 5: Exergy eestruction and efficiency in each component.

Equipment, k		Exergy destruction (kW)	Exergy efficiency (%)
104-E-101	Heat exchanger	636.5	78.85
105-E-101	Heat exchanger	1208.92	89.30
105-E-102	Heat exchanger	540.55	90.25
105-E-106	Heat exchanger	77.62	76.95
104-E-107	Heat exchanger	35.15	85.50
111-A-101	Air cooler	1482.95	76.95
105-K-101	Compressor	666.37	74.10
111-K-101/1st	Compressor	204.74	69.35
111-K-101/2nd	Compressor	798.22	72.20
105-X-101	Expander	998.02	71.25
V-1	Expansion valve	368.6	17.10
V-3	Expansion valve	19.95	56.05
V-4	Expansion valve	21.95	52.25
V-6	Expansion valve	126.92	59.85
V-7	Expansion valve	691.6	28.50

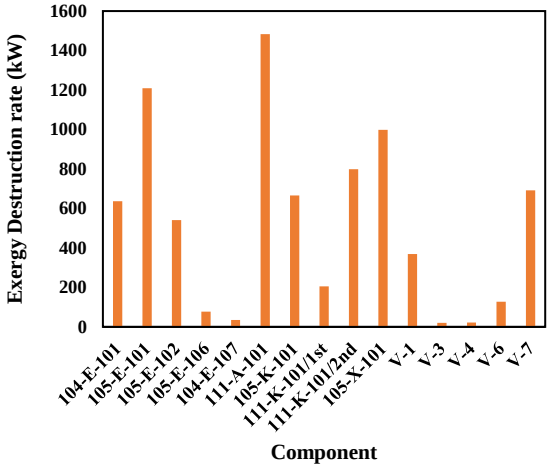

Fig. 8: Different parts of exergy destruction of process components.

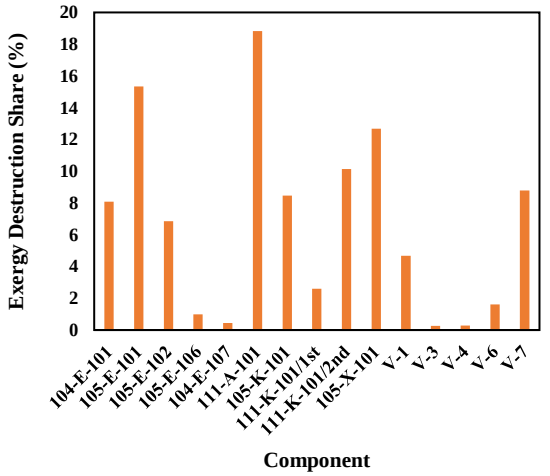

Fig. 9: Different parts of exergy destruction share of process components.

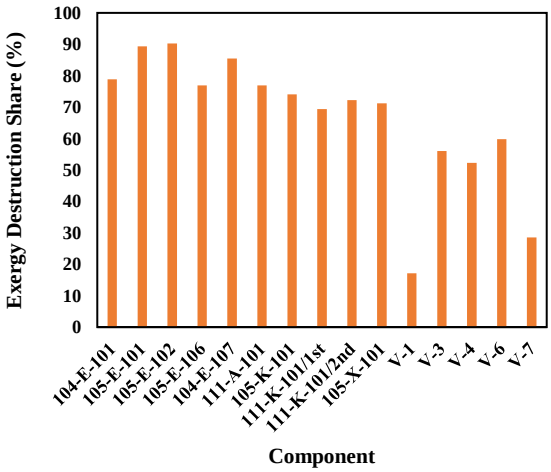

Fig. 10: Different parts of exergy efficiency of each component.

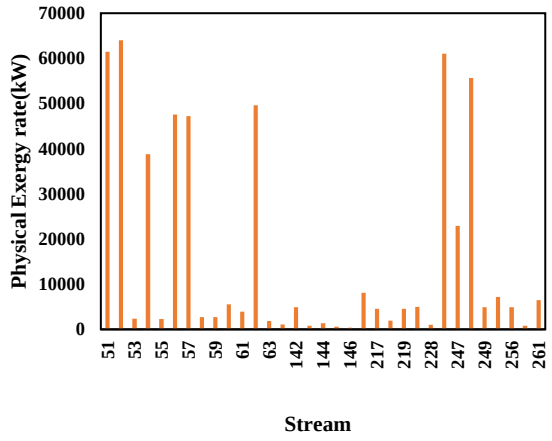

Fig. 11: Rate of physical exergy in each component.

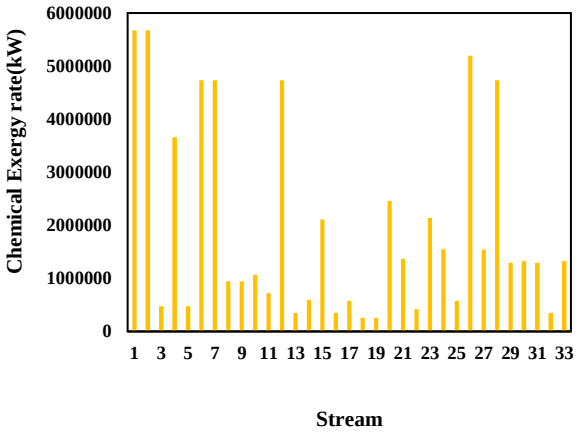

Fig. 12: Rate of chemical exergy in each component.

Figs. 11 and 12 also show the chemical and physical exergy rates in each component.

Exergoeconomic analysis

Exergoeconomic provides information for system design that is not possible through conventional energy analysis and economic evaluation by analyzing energy and economic principles. In energy systems, economic analysis and improvement, annual investment, fuel cost, and system maintenance cost must be calculated. In this paper, the Total Revenue Requirement (TRR) method, as developed by the Electricity Research Institute [33], is used to analyze the system economically (see Table 7).

Table 6: Exergy destruction details.

	$E_{END;K}$	$E_{EXD;K}$	$E_{UND;K}$	$E_{AVD;K}$	$E_{END;K;AV}$	$E_{END;K;UN}$	$E_{EXD;K;AV}$	$E_{EXD;K;UN}$
104-E-101	342.9	313.7	515.48	141.12	75.11	266.32	69.34	245.82
105-E-101	768.88	478.22	719.86	527.24	327.1	433.61	209.13	277.22
105-E-102	476.74	80.88	446.88	110.74	94.8	379.18	16.73	66.91
105-E-106	40.96	39.09	52.43	27.64	14.29	26.54	13.73	25.5
105-E-107	24.63	11.62	18.91	17.35	11.65	12.63	5.74	6.21
111-A-101	877.43	652.57	1063.74	466.26	270.34	601.75	203.95	453.95
105-K-101	512.98	174.44	295.41	392	289.95	218.74	101.87	76.85
111-K-101/1	139.44	71.77	68.6	142.61	94.79	44.6	48.82	22.97
111-K-101/2	636.24	186.96	266.56	556.64	431.02	202.83	128.74	60.58
105-X-101	769.16	260.38	582.12	447.42	335.21	426.63	117.78	149.9

Table 7: Exergy and unit exergy cost for each stream of MFC configuration.

Stream	C ($/GJ)	Stream	C ($/GJ)
51	20.08	145	20.06
52	19.61	146	18.84
53	19.96	149	18.89
54	20.87	217	21.65
55	19.76	218	79.76
56	20.98	219	84.64
57	20.21	220	72.4
58	20.18	228	85.16
59	18.92	244	85.08
60	20.27	247	81.85
61	17.66	248	76.74
62	19.45	249	80.11
63	19.09	250	80.93
64	21.3	256	102.9
142	19.96	257	108.87
143	18.17	261	98.63
144	20.75	-	-

Table 8: Economic constants and assumptions.

Economic parameters	Value
The average annual rate of the cost of money (i_{eff})	10%
Average nominal inflation rate for the operating and maintenance cost (r_{OMC})	5%
Average nominal inflation rate for fuel (r_{FC})	5%
Plant economic life (life spawn)	25 years
Total annual operating hours of the system operation at full load	7300

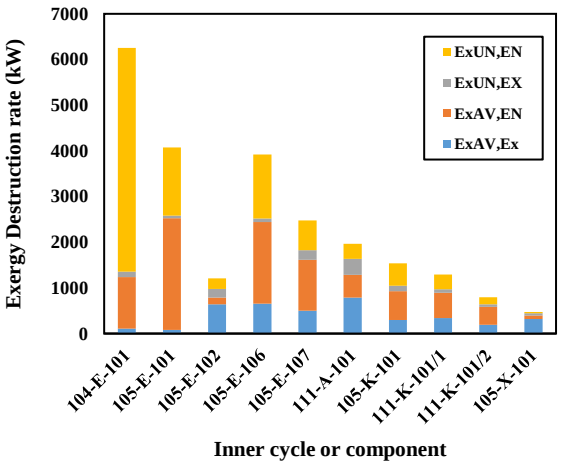

Fig. 13: Different parts of exergy degradation of process equipment.

In this method, all costs, including return on investment, are calculated. Based on the assumptions of Table 8, equipment and fuel prices and total annual revenue are calculated. Finally, all costs, including maintenance and fuel costs, are balanced during system operation. As the years of system operation increase, investment costs decrease, while fuel costs increase. Therefore, the amount of the required total annual income balance (TRRL) is calculated by the return on investment factor (CRF) and monetary depreciation given in Equation (15) [35]:

$$TRR_L = CRF \sum_{1}^{BL} \frac{TRR_j}{(1+i_{eff})_j} \quad (15)$$

TRRj represents the total revenue required in the fourth year of system operation, and *BL* represents the system's economic life cycle as measured in years. i_{eff} is the average annual rate of effective depreciation. The return on equity (*CRF*) is calculated as follows:

$$CRF = \frac{i_{eff}(1+i_{eff})^{BL}}{(1+i_{eff})^{BL}-1} \quad (16)$$

In this study, the TRRj is the sum of four annual values, including the minimum Return on Investment (ROI), the total return on investment (TCR), Operating and Maintenance Costs (OMC), and Fuel Costs (FC).

The equations for estimating the equipment's cost are illustrated in Table 9 and the results calculated are illustrated in Table 10.

There is more than one unknown variable for some types of equipment with more than one output flux, so the auxiliary equations are determined according to P and F [19] for these types of equipment. Tables 8 and 9 show the cost balance and auxiliary model of a system, respectively. Given that the equations are not solved independently for some components, a set of linear-dependent equations must be solved simultaneously. A computer program has been developed in MATLAB to solve the cost equilibrium and auxiliary equations to obtain the unit surplus cost per stream, as shown in Table 10.

Fig. 14 shows the advanced exergy destruction cost analysis of the process equipment under study. The destructive exergy of process equipment is divided into four categories: avoidable - endogenous/exogenous and unavoidable - endogenous/exogenous, and the values of each part are specified in Fig. 14. In the 104-E-101 heat exchanger, the inaccessible destructive exergy is more than the available part, while in the other components, the destructive exergy is more than the inaccessible part. Also, except for 105-X-101, 105-K-101, 111-K-101/2, 111-A-101, and 105-E-102, in the other components, the endogenous destructive energy is greater than the exogenous part, indicating that in these components, the most source of irreversibility is the components themselves, not the components themselves.

Table 9: Thermoeconomic cost model.

Equipment	Purchased equipment cost functions
Compressor	$C_C = 7.90(HP)^{0.62}$ C_C= Cost of Compressor (k$)
Heat exchanger	$C = 1.218 f_d f_m f_p C_b$ $C_b = \exp[8.821 - 0.30863(\ln A) + 0.0681(\ln A)^2]$, 150<A<12000, $f_d = \exp(-1.1156 + 0.0906 \ln A)$, f_M= Material Factor, f_P=Pressure factor
Separator	$C = 1.218[a + bW]$, K$ 5<W a= 42, b=1.63
Air cooler	$C_{AC} = 1.218 f_m f_P \exp[a + b\ln Q + c(\ln Q)^2]$, Q in KSCFM C_{AC}= Cost of Air cooler (k$) f_m=Material Factor, f_P=Pressure Factor, a=0.4692, b=0.1203, c=0.0931
Turbo Expander	$C_{TE} = 0.378(HP)^{0.81}$ C_{TE}= Cost of Turbo Expander (k$)
Absorption	$C_T = 1.218[f_1 C_b + N f_2 f_3 f_4 C_t + C_{p1}]$ $C_t = 457.7 \exp(0.1739D)$, 2<D $C_b = 1.218 \exp[6.629 + 0.1826(\ln W) + 0.02297(\ln W)^2]$, 4250<W<980,000 lb shell $C_{p1} = 300 D^{0.7396} L^{0.7068}$, 3<D<21, 27<L f_1= Material Factor, $f_2 = 1.189 + 0.0577D$, f_3=Tray Types Factor, $f4 = \frac{2.25}{(1.0414)^N}$

Table 10: Results of exergoeconomic study.

Component	$\dot{E}_D$ (kW)	C_F ($/GJ)	C_P ($/GJ)	$\dot{C}_D$ ($/hr)	$\dot{Z}$ ($/hr)	E (%)	Y_D(%)	r(%)	f (%)
104-E-101	2006.63	20.07	37.9	18.38	133.43	68.44	6.79	35.43	92.31
105-E-101	5021.86	19.87	30.05	10.7	340.18	71.61	5.21	35.83	96.65
105-E-102	2266.2	19.21	32.54	11.21	184.41	78.33	7.98	34.46	97.89
105-E-106	3904.04	19.54	30.43	11.13	246.3	74.29	6.07	35.42	86.77
105-E-107	397.04	19	36.72	19.23	59.86	70.29	12.83	30.31	71.83
111-A-101	1751.32	17.92	31.03	14.44	143.8	71.54	8.59	38.53	84.87
105-K-101	4702.1	18.4	26.86	10.72	284.25	76.94	6.14	35.7	98.7
111-K-101/1	1019.05	11.05	18.94	7.94	17.63	65.5	1.46	34.43	68.08
111-K-101/2	719.03	17.8	20.18	0.42	3.62	97.42	0.53	49.73	86.35
105-X-101	810.49	20.03	20.43	0.43	3.78	94.83	0.45	49.34	88.16

The cost of destructive exergy of process equipment is divided into four categories: avoidable - endogenous/exogenous and unavoidable - endogenous/exogenous, and the percentage of the impact of each part is specified in the figure. In the 104-E-101 heat exchanger, the cost of unavailable destructive exergy is higher than available, while in the other components, the cost of available destructive exergy is higher than unavailable. Also, except for 105-X-101, 105-K-101, 111-K-101/2, 111-A-101, and 105-E-102 in other components, the cost of endogenous energy destruction is higher than the external part. Besides, in 104-E-101 converters and 105-E-101 compressors 105-E-106, because the cost of endogenous destructive energy is available at a high rate, increasing their efficiency will significantly reduce returns (see Fig. 15).

The investment cost of process equipment is divided into four categories: avoidable - endogenous/exogenous and unavoidable - endogenous/exogenous, and the percentage of the impact of each part on the figure is specified. As can be seen, except for 105-E-102 and 111-A-101, where the exogenous part's investment cost is more

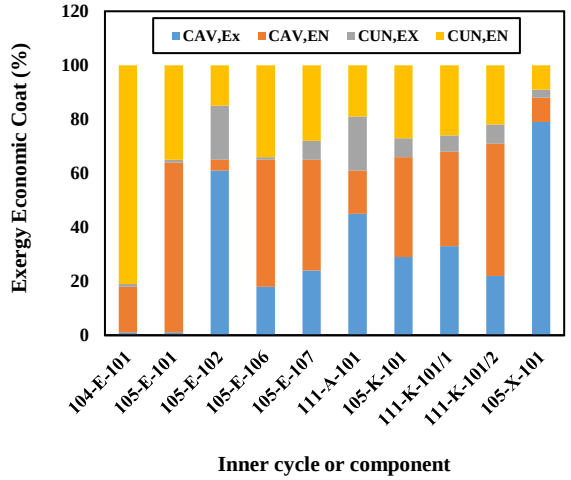

Fig. 14: the analysis of the advanced exergoeconomic cost analysis of the process equipment under study.

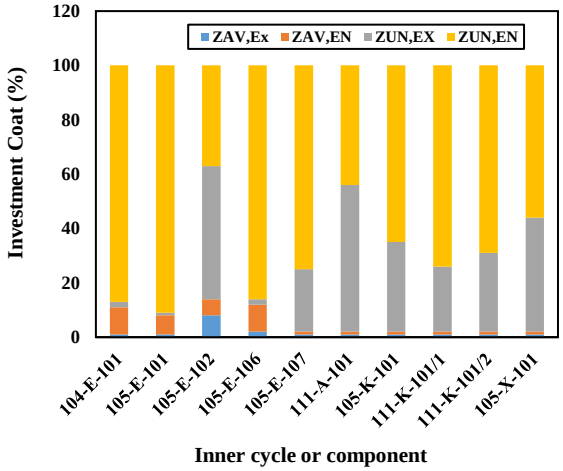

Fig. 15: Advanced investment cost analysis of process equipment.

than the endogenous part, in other types of equipment, the endogenous part's investment cost is more than the exogenous part. Also, in all components, the inaccessible part's investment cost is more than the available part. Besides, given the high cost of advanced endogenous investment in 104-E-101 converters and 105-E-101, 105-E-106 compressors, there is a good potential for improving their performance by increasing efficiency, which can be reduced[41-45].

Three strategies are considered to reduce the cost of available destructive exergy. When the amount of destructive exergy available is large, there is good potential for improving system performance. As a result, strategy (a) can be used in this case. Strategy (b) is used when the cost of exogenous destructive exergy at hand is significant compared to the available endogenous portion. It should be noted that except for 105-E-101 and 104-E-101, other process types of equipment have this feature, and this strategy can be used for them. Finally, strategy (c) is used when the cost of the exogenous destructive energy available is substantial and at least half of the total cost of the destructive energy is available. As it turns out, strategy C can be used for the 105-E-102, 111-A-101, 105-X-101, 105-K-101, and 111-K-101/2 components.

Advanced exergy and exo-economic analysis have been performed on the integrated process of natural liquefied natural gas (LNG) production and Natural gas condensate (NGL). The results of the process analysis are as follows:

- Based on the cost of endogenous destructive exergy at hand, 104-E-101, 105-E-101, and 105-E-106 have higher values than other equipment types. Also, the 105-E-101 heat exchanger has the highest amount of endogenous destructive energy in hand, which increases the efficiency of this equipment and greatly reduces this amount.
- The available endogenous destructive investment cost results show that 104-E-101 converter and 105-E-101, 105-E-106 compressors can improve their performance efficiency in this field. It should be noted that 105-E-106 and 105-E-101 compressors have the highest amount of endogenous destructive investment available among the types of equipment available, respectively. Also, the studied air conditioners have the lowest amount of endogenous destructive investment available.
- On the whole, and based on the results of the total cost of endogenous destructive exergy at hand, the 104-E-101 heat exchanger is the priority of choice for performance modification.
- The simulation shows that the equivalent of 1549.59 barrels per day of GTL products can be produced, always the selling price of products, bank profits, inflation, etc. have a significant impact on the output of economic evaluation, as well as the carbon tax and its increase tax on pollution, the environment of industries, etc., and rising global oil and gas prices, will greatly contribute to the operation of this project [19, 36-39].

CONCLUSIONS

According to the simulation, using the GTL unit with the Flare gas input feed of the sample refinery can produce 1549 barrels per day, which shows Flare gas's ability to be used in industry. Compared to the information obtained from Parsian Refinery Flare Gas, which is estimated to produce 536 barrels of GTL per day, or Assaluyeh Refinery, which is estimated to cost 48056 barrels of GTL per day, according to Flare Gas data collected before 2012. In this case, the accumulation of flare gases and its high production capacity can be a deterrent to the implementation of such projects because it requires a large volume of investment and also identifying suitable land for the construction of GTL units, if for low capacity in addition to low Investment volume, etc. More companies can participate in such tenders and compete, which will enable domestic companies to enter this field, including Sarv Oil and Gas Company, which with a lot of effort is one of the few companies with GTL technical knowledge - Given the lifespan of GTL units, which is about 25 to 35 years. With the added value created by the gases released into the atmosphere, the return on investment is less than five years, but it is still important to use flare gas. Several Flare gas recovery methods should be examined from a technical and economic point of view in a set. In this regard, the economic evaluation of those methods is an integral part of the research and compares methods technically, a method in which more application and a more appropriate output can be used. Besides, the conclusion for choosing the appropriate method is based on the output of the economic evaluation. However, this method and similar methods of recovering flare gases will greatly help improve the state of the environment, including reducing pollutants and toxic substances around the industrial environment and their impact on the planet. Taking into account the special environmental conditions, global warming, and climate change that have caused economic and health damage to the international community, as well as following the Tokyo Accords, etc., according to the commitment of most countries, including Iran, Any method that has an economic aspect, to take big steps, whether it is a method of creating a cycle for reuse in the same industrial environment or to become a new material or force to produce new work or product in near or far consumption, which eventually The positive economic effects of Flare gas recycling methods will also be reflected in the country's turnover.

Nomenclature

NGN	Natural gas to liquid
LNG	Liquified natural gas
C	Cost rate, $/h
C_D	Cost rate of exergy destruction, $/h
Ex	Exergy rate, kW
m	Mass flow rate, kg/s
W	Work rate, kW
Z	Investment, operation, and maintenance cost rate, $/h
c	Cost per exergy unit, $/GJ
c_F	Unit cost of the fuel, $/GJ
c_P	Unit cost of the product, $/GJ
e	Specific exergy, kJ/kg
E	Heat exchanger
F	Fuel
FT	Fischer–Tropsch
LHV	Lower heating value
MMSCFD	Million standard cubic feet per day
Ph	Physical
f	Exergoeconomic factor, %
h	Specific enthalpy, kJ/kg
I	Irreversibility or exergy destruction, kW
P	Pressure, kPa
r	Relative cost difference, %
s	Specific entropy, kJ/kg-C
T	Temperature, °C
x	Mole fraction
ε	Exergetic efficiency, %
φ	Maintenance factor
o	Reference state
A	Air cooler
ACo	Air compressor
ch	Chemical
CRF	Capital recovery factor
D	Destruction
P	Product

Received : Jun. 2, 2021 ; Accepted : Sept. 20, 2021

References

[1] Bejan A., Tsatsaronis G., Moran M., Thermal Design and Optimization, John Wiley & Sons, Inc. (1996).

[2] Elliot D., Huang S., Chen J.J., Lee R.J., Yao J., Zhang Y., Benefits of Integrating NGL Extraction and LNG liquefaction Technology, *AIChE Journal*., (2005).

[3] Ahmadi N., Rezazadeh S., Dadvand A., Mirzaee I., Study of the Effect of Gas Channels Geometry on the Performance of Polymer Electrolyte Membrane Fuel Cell, *Periodica Polytechnica Chemical Engineering*, **62(1)**: 97-105 (2018).

[4] Ahmadi N., Rezazadeh S., Dadvand A., Mirzaee I., Modelling of Gas Transport in Proton Exchange Membrane Fuel Cells, *Proceedings of the Institution of Civil Engineers-Energy*, **170(4)**: 163-179 (2017).

[5] Ahmadi N., Kõrgesaar M., Analytical Approach to Investigate the Effect of Gas Channel Draft Angle on the Performance of PEMFC and Species Distribution, *International Journal of Heat and Mass Transfer*, **152**: - (2020).

[6] Finn A.J., Developments in Natural Gas Liquefaction, *Hydrocarbon Process*, 47−59 (1999).

[7] Norouzi, N. The Pahlev Reliability Index: A Measurement for the Resilience of Power Generation Technologies Versus Climate Change, *Nuclear Engineering and Technology* (2020).

[8] Norouzi N., Fani M., Talebi S. Exergetic Design and Analysis of a Nuclear SMR Reactor Tetrageneration (Combined Water, Heat, Power, and Chemicals) with Designed PCM Energy Storage and a CO_2 Gas Turbine Inner Cycle, *Nuclear Engineering and Technology*, **53**: 677–687 (2021).

[9] Norouzi N., Hosseinpour M., Talebi S., Fani M., A 4E Analysis of Renewable Formic Acid Synthesis from the Electrochemical Reduction of Carbon Dioxide and Water: Studying Impacts of the Anolyte Material on the Performance of the Process, *Journal of Cleaner Production*, **293**, (2021).

[10] Khajehpour H., Norouzi N., Shiva N., Folourdi R. M., Bahremani E. H., Exergy Analysis and Optimization of Natural Gas Liquids Recovery Unit, *International Journal of Air-Conditioning and Refrigeration*, **29**: (2021).

[11] Norouzi N., Shiva N., Khajehpour H., Optimization of Energy Consumption in the Process of Dehumidification of Natural Gas, *Biointerface Research in Applied Chemistry*, **11**: 14634–14639 (2021).

[12] Norouzi N., Talebi S., Fani M., Khajehpour H., Exergy and Exergoeconomic Analysis of Hydrogen and Power Cogeneration Using an HTR Plant, *Nuclear Engineering and Technology* (2021).

[13] Norouzi N., Khajehpour H., Simulation of Methane Gas Production Process from Animal Waste in a Discontinuous Bioreactor, *Biointerface Research in Applied Chemistry*, **11**: 13850–13859 (2021).

[14] Norouzi N., Talebi S., Najafi P. Thermal-hydraulic Efficiency of a Modular Reactor Power Plant by Using the Second Law of Thermodynamic, *Annals of Nuclear Energy*, **151**: - (2021).

[15] Khajehpour H., Norouzi N., Fani M., An Exergetic Model for the Ambient Air Temperature Impacts on the Combined Power Plants and its Management Using the Genetic Algorithm, *International Journal of Air-Conditioning and Refrigeration*, **29** (2021).

[16] Fani M., Norouzi N., Ramezani M., Energy, Exergy, and Exergoeconomic Analysis of Solar Thermal Power Plant Hybrid with Designed PCM Storage, *International Journal of Air-Conditioning and Refrigeration*, **28**: (2020).

[17] Gallo W.L., Gallego A.G., Acevedo V.L., Dias R., Ortiz H.Y., Valente B.A., Exergy Analysis of the Compression Systems and its Prime Movers for a FPSO Unit, *Journal of Natural Gas Science and Engineering*, **44**: 287–298 (2017).

[18] Arnaiz del Pozo C., Jiménez Álvaro Á., Rodríguez Martín J., López Paniagua I. Efficiency Evaluation of Closed and Open Cycle Pure Refrigerant Cascade Natural Gas Liquefaction Process Through Exergy Analysis, *Journal of Natural Gas Science and Engineering*, **89**: (2021).

[19] Ghorbani B., Ebrahimi A., Rooholamini S., Ziabasharhagh M. Pinch and Exergy Evaluation of Kalina/Rankine/Gas/Steam Combined Power Cycles for Tri-Generation of Power, Cooling and Hot Water Using Liquefied Natural Gas Regasification, *Energy Conversion and Management*, **223**: 113328 (2020).

[20] Zhang S., Jiang H., Jing J., Qin M., Chen D., Chen C., Comprehensive Comparison of Enhanced Recycle Split Vapour Processes for Ethane Recovery, *Energy Reports*, **6**: 1819–1837 (2020).

[21] Mehrpooya M., Vatani A., Moosavian S. Optimum Pressure Distribution in Design of Cryogenic NGL Recovery Processes, *Iran. J. Chem. Chem. Eng. (IJCCE)*, **31(3)**: 97-109 (2012).

[22] Ahmadi S., Nasr R. Comparative Study and Multi-Objective Optimization of Various Configurations in Natural Gas Liquefaction Process, *Iran. J. Chem. Chem. Eng. (IJCCE)*, **39(1)**: 313-336 (2020).

[23] Azari A., Shariaty-Niassar M., Alborzi M. Short-term and Medium-term Gas Demand Load Forecasting by Neural Networks, *Iran. J. Chem. Chem. Eng. (IJCCE)*, **31(4)**: 77-84 (2012).

[24] Norouzi N., 4E Analysis and Design of a Combined Cycle with a Geothermal Condensing System in Iranian Moghan Diesel Power Plant, *International Journal of Air-Conditioning and Refrigeration*, **28**: (2020).

[25] Garousi Farshi L., Mahmoudi S.M.S., Rosen M.A., Exergoeconomic Comparison of Double Effect and Combined Ejector-double Effect Absorption Refrigeration Systems, *Applied Energy*, **103**: 700–711 (2013).

[26] Ghorbani B., Salehi G.R., Amidpour M., Hamedi M.H., Exergy and Exergoeconomic Evaluation of Gas Separation Process, *Journal of Natural Gas Science and Engineering*, **9**: 86-93 (2012).

[27] Morosuk T., Tesch S., Hiemann A., Tsatsaronis G., Bin Omar N., Evaluation of the PRICO Liquefaction Process using Exergy-based Methods, *Journal of Natural Gas Science and Engineering*, 1-9 (2015).

[28] Siddiqui F.R., El-Shaarawi M.A.I., Said S.A.M, Exergoeconomic Analysis of a Solar Driven Hybrid Storage Absorption Refrigeration Cycle, *Energy Conversion and Management*, **80**: 165-172 (2014).

[29] Vatani A., Mehrpooya M., Palizdar A., Energy and Exergy Analyses of Five Conventional Liquefied Natural Gas Processes, *International Journal of Energy Research*, **38**: 1843-1863 (2014).

[30] Azizkhani A., Gandomkar A., A Novel Method for Application o Nanoparticles as Direct Asphaltene Inhibitors During Miscible CO2 Injection, *Journal of Petroleum Science and Engineering*, **185**: (2020).

[31] Pellegrini L.A., De Guido G., Valentina V., Energy and Exergy Analysis of Acid Gas Removal Processes in the LNG Production Chain, *Journal of Natural Gas Science and Engineering*, **61**: 303–319 (2019).

[32] Najibullah Khan N. B., Barifcani A., Tade M., Pareek V., A Case Study: Application of Energy and Exergy Analysis for Enhancing the Process Efficiency of a Three Stage Propane Pre-Cooling Cycle of the Cascade LNG Process, *Journal of Natural Gas Science and Engineering*, **29**: 125–133 (2016).

[33] Ghorbani B., Salehi G.R., Ghaemmaleki H., Amidpour M., Hamedi M.H., Simulation and Optimization of Refrigeration Cycle in NGL Recovery Plants with Exergy-Pinch Analysis, *Journal of Natural Gas Science and Engineering*, **7**: 35–43 (2012).

[34] Bidar B., Shahraki F. Energy and Exergo-Economic Assessments of Gas Turbine Based CHP Systems: A Case Study of SPGC Utility Plant, *Iran. J. Chem. Chem. Eng. (IJCCE)*, **37(5)**: 209-223 (2018).

[35] Noorpoor A., Mazare F. Conventional and Advanced Exergetic and Exergoeconomic Analysis Applied to an Air Preheater System for Fired Heater (Case Study: Tehran Oil Refinery Company), *Iran. J. Chem. Chem. Eng. (IJCCE)*, **37(4)**: 205-219 (2018).

[36] Khoshrou I., Jafari Nasr M., Bakhtari K., Exergy Analysis of the Optimized MSFD Type of Brackish Water Desalination Process, *Iran. J. Chem. Chem. Eng. (IJCCE)*, **36(6)**: 191-208 (2017).

[37] Norouzi N., 4E Analysis of a Fuel Cell and Gas Turbine Hybrid Energy System, *Biointerface Research in Applied Chemistry*, **11**: 7568-7579 (2021).

[38] Zaresharif M., Vatani A., Ghasemian M., Evaluation of Different Flare Gas Recovery Alternatives with Exergy and Exergoeconomic Analyses, *Arabian Journal for Science and Engineering*: 1-20 (2021).

[39] Hajizadeh A., Mohamadi-Baghmolaei M., Azin R., Osfouri S., Heydari I., Technical and Economic Evaluation of Flare Gas Recovery in a Giant Gas Refinery, *Chemical Engineering Research and Design*, **131(1)**: 506-519 (2018).

[40] Sabbagh O., Fanaei M.A., Arjomand A., Optimal Design of a Novel NGL/LNG Integrated Scheme: Economic and Exergetic Evaluation, *Journal of Thermal Analysis and Calorimetry*, **18**:1-6 (2020).

[41] Abdulrahman I., Máša V., Teng S.Y., Process Intensification in The Oil and Gas Industry: A Technological Framework, *Chemical Engineering and Processing-Process Intensification*, **2**: 108208 (2020).

[42] Norouzi N., Talebi S., Fabi M., Khajehpour H., Heavy Oil Thermal Conversion and Refinement to the Green Petroleum: A Petrochemical Refinement Plant Using the Sustainable Formic Acid for the Process, *Biointerface Research in Applied Chemistry*, **10**: 6088 - 6100 (2020).

[43] Norouzi N., Kalantari G., Talebi S., Combination of Renewable Energy in the Refinery, with Carbon Emissions Approach, *Biointerface Research in Applied Chemistry*, **10**: 5780-5786 (2020).

[44] Khajehpour H., Norouzi N., Bashash Jafarabadi Z., Valizadeh G., Hemmati M., Energy, Exergy, and Exergoeconomic (3E) Analysis of Gas Liquefaction And Gas Associated Liquids Recovery Co-Process Based on the Mixed Fluid Cascade Refrigeration Systems, *Iran. J. Chem. Chem. Eng. (IJCCE)*, **41(4):** 1391-1402 (2022).

[45] Norouzi N., Talebi S. Exergy, Economical and Environmental Analysis of a Natural Gas Direct Chemical Looping Carbon Capture and Formic Acid-Based Hydrogen Storage System, *Iran. J. Chem. Chem. Eng. (IJCCE)*, (2021) [in Press].

[46] Norouzi N. Hydrogen Production in the Light of Sustainability: A Comparative Study on the Hydrogen Production Technologies Using the Sustainability Index Assessment Method, *Nuclear Engineering and Technology*, **54(4)**: 1288-1294 (2021).

[47] Vessally E., Mohammadi S., Abdoli M., Hosseinian A., Ojaghloo P., Convenient and Robust Metal-Free Synthesis of Benzazole-2-Ones Through the Reaction of Aniline Derivatives and Sodium Cyanate in Aqueous Medium, *Iran. J. Chem. Chem. Eng. (IJCCE)*, **39(5)**: 11-19 (2020).

[48] Gharibzadeh F., Vessally E., Edjlali L., Es'haghi M., Mohammadi R., A DFT Study on Sumanene, Corannulene and Nanosheet as the Anodes in Li−Ion Batteries, *Iran. J. Chem. Chem. Eng. (IJCCE)*, **39(6)**: 51-62 (2020).

[49] Afshar M., Khojasteh R.R., Ahmadi R., Nakhaei Moghaddam M., In Silico Adsorption of Lomustin Anticancer Drug on the Surface of Boron Nitride Nanotube, *Chem. Rev. Lett.*, **4**: 178-184 (2021).

[50] Mohammad Alipour F., Babazadeh M., Vessally E., Hosseinian, A., Delir Kheirollahi Nezhad P., A Computational Study on the Some Small Graphene-Like Nanostructures as the Anodes in Na−Ion Batteries, *Iran. J. Chem. Chem. Eng. (IJCCE)*, **40(3)**: 691-703 (2021).

[51] Hashemzadeh B., Edjlali L., Delir Kheirollahi Nezhad P., Vessally E., A DFT Studies on a Potential Anode Compound for Li-Ion Batteries: Hexa-Cata-Hexabenzocoronene Nanographen, *Chem. Rev. Lett.*, **4**: 232-238 (2021).

[52] Vessally E., Farajzadeh P., Najafi E., Possible Sensing Ability of Boron Nitride Nanosheet and its Al– and Si–Doped Derivatives for Methimazole Drug by Computational Study, *Iran. J. Chem. Chem. Eng. (IJCCE)*, **40 (4)**: 1001-1011 (2021).

[53] Majedi S., Sreerama L., Vessally E., Behmagham F., Metal-Free Regioselective Thiocyanation of (Hetero) Aromatic C-H Bonds using Ammonium Thiocyanate: An Overview, *J. Chem. Lett.*, **1**: 25-31 (2020).

[54] Amani V., Zakeri M., Ahmadi R., Binuclear Nickel(II) Complex Containing 6-methyl-2,2'-bipyridine and Chloride Ligands: Synthesis, Characterization, Thermal Analyses, and Crystal Structure Determination, *Iran. J. Chem. Chem. Eng. (IJCCE)*, **39(2)**: 113-122 (2020).

[55] Salehi N., Vessally E., Edjlali L., Alkorta I., Eshaghi M., Nan@Tetracyanoethylene (n=1-4) systems: Sodium salt vs Sodium Electride, *Chem. Rev. Lett.*, **3**: 207-217 (2020).

[56] Soleimani-Amiri S., Asadbeigi N., Badragheh S., A Theoretical Approach to New Triplet and Quintet (nitrenoethynyl) alkylmethylenes,(nitrenoethynyl) alkylsilylenes,(nitrenoethynyl) alkylgermylenes, *Iran. J. Chem. Chem. Eng. (IJCCE)*, **39(4)**: 39-52 (2020).

[57] Sreerama L., Vessally E., Behmagham F., Oxidative Lactamization of Amino Alcohols: An Overview, *J. Chem. Lett.*, **1**: 9-18 (2020).

[58] Kamel M., Mohammadifard M., Thermodynamic and Reactivity Descriptors Studies on the Interaction of Flutamide Anticancer Drug with Nucleobases: A Computational View, *Chem. Rev. Lett.*, **4**: 54-65 (2021).

[59] Vessally E., Musavi M., Poor Heravi M.R., A Density Functional Theory Study of Adsorption Ethionamide on the Surface of the Pristine, Si and Ga and Al-Doped Graphene, *Iran. J. Chem. Chem. Eng. (IJCCE)*, **40(6)**: 1720-1736 (2021).

[60] Vakili M., Bahramzadeh V., Vakili M., A Comparative Study of SCN- Adsorption on the $Al_{12}N_{12}$, $Al_{12}P_{12}$, and Si and Ge -doped $Al_{12}N_{12}$ Nano-Cages to Remove from the Environment, *J. Chem. Lett.*, **1**: 172-178 (2020).

[61] Mosavi, M., Adsorption behavior of Mephentermine on the Pristine and Si, Al, Ga- Doped Boron Nitride Nanosheets: DFT Studies, *J. Chem. Lett.*, **1**: 164-171 (2020).

[62] Vessally E., Siadati S.A., Hosseinian A., Edjlali L., Selective Sensing of Ozone and the Chemically Active Gaseous Species of the Troposphere by Using the C20 Fullerene and Graphene Segment, *Talanta*, **162**: 505-510 (2017).

[63] Rabipour S., Mahmood E.A., Afsharkhas M., Abbasi V., A Review on the Cannabinoids Impacts on Psychiatric Disorders, *Chem. Rev. Lett.*, **5**: 234-240 (2022).

[64] Siadati S.A., Vessally E., Hosseinian A., Edjlali L., Possibility of Sensing, Adsorbing, and Destructing the Tabun-2D-skeletal (Tabun nerve agent) by C20 Fullerene and its Boron and Nitrogen Doped Derivatives, *Synthetic Metals*, **220**: 606-611 (2016).

[65] Rabipour S., Mahmood E.A., Afsharkhas M., Medicinal Use of Marijuana and its Impacts on Respiratory System, *J. Chem. Lett.*, **3**: 86-94 (2022).

[66] Cao Y., Soleimani-Amiri S., Ahmadi R., Issakhov A., Ebadi A.G., Vessally E., Alkoxysulfenylation of Alkenes: Development and Recent Advances, *RSC Advances*, **11**: 32513-32525 (2021).

[67] Vessally E., Soleimani-Amiri S., Hosseinian A., Edjlali L., Babazadeh M., Chemical Fixation of CO_2 to 2-aminobenzonitriles: A Straightforward Route to Quinazoline-2, 4 (1H, 3H)-Diones with Green and Sustainable Chemistry Perspectives, *J. CO_2 Util.*, **21**: 342-352 (2017).

[68] Arshadi S., Vessally E., Hosseinian A., Soleimani-Amiri S., Edjlali L., Three-Component Coupling of CO_2, Propargyl Alcohols, and Amines: An Environmentally Benign Access to Cyclic and Acyclic Carbamates (A Review), *J. CO_2 Util.*, **21**: 108-118 (2017).

[69] Kassaee M.Z., Buazar F., Soleimani-Amiri S., Triplet Germylenes with Separable Minima at ab Initio and DFT Levels, *Journal of Molecular Structure: THEOCHEM*, **866(1-3)**: 52-57 (2008).

[70] Kassaee M.Z., Aref Rad H., Soleimani Amiri S., Carbon–Nitrogen Nanorings and Nanoribbons: A Theoretical Approach for Altering the Ground States of Cyclacenes and Polyacenes, *Monatshefte für Chemie-Chemical Monthly*, **141(12)**: 1313-1319 (2010).

[71] Koohi M., Soleimani Amiri S., Haerizade B.N., Substituent Effect on Structure, Stability, and Aromaticity of Novel BnNmC20–(n+ m) Heterofullerenes, *Journal of Physical Organic Chemistry*, **30(11)**: e3682 (2017).

[72] Koohi M., Soleimani-Amiri S., Shariati M. Novel X-and Y-substituted Heterofullerenes X 4 Y 4 C 12 Developed from the Nanocage C 20, where X= B, Al, Ga, Si and Y= N, P, As, Ge: a Comparative Investigation on their Structural, Stability, and Electronic Properties at DFT, *Structural Chemistry*, **29(3)**: 909-920 (2018).

[73] Soleimani- Amiri S., Singlet and Triplet Cyclonona-3, 5, 7- trienylidenes and their α, ά- halogenated Derivatives at DFT, *Journal of Physical Organic Chemistry*, **33(2)**: e4018 (2020).

[74] Soleimani-Amiri, S., Asadbeigi, N., Badragheh, S. A Theoretical Approach to New Triplet and Quintet (nitrenoethynyl) alkylmethylenes,(nitrenoethynyl) alkylsilylenes,(nitrenoethynyl) alkylgermylenes. Iran. J. Chem. Chem. Eng., 39(4): 39-52 (2020).

[75] Soleimani-Amiri, S. Identification of Structural, Spectroscopic, and Electronic Analysis of Synthesized 4-(5-Phenyl-1, 3, 4-Oxadiazol-2-Ylthio)-3-Methylbenzene-1, 2-Diol: A Theoretical Approach, *Polycyclic Aromat. Compd*, **41(3)**: 635-652 (2021).

[76] Poor Heravi M.R., Azizi B., Abdulkareem Mahmood E., Ebadi A.G., Ansari M.J., Soleimani-Amiri S., Molecular Simulation of the Paracetamol Drug Interaction with Pt-decorated BC3 Graphene-Like Nanosheet, *Molecular Simulation*, **48(6)**: 517-525 (2022).

[77] Ghazvini M., Sheikholeslami-Farahani F., Soleimani-Amiri S., Salimifard M., Rostamian R., Green Synthesis of Pyrido [2, 1-a] isoquinolines and Pyrido [1, 2-a] Quinolines by Using ZnO Nanoparticles, *Synlett*, **29(04)**: 493-496 (2018).

[78] Soleimani- Amiri S., Shafaei F., Varasteh Moradi A., Gholami- Orimi F., Rostami Z., A Novel Synthesis and Antioxidant Evaluation of Functionalized [1, 3]-Oxazoles Using Fe_3O_4- Magnetic Nanoparticles. *Journal of Heterocyclic Chemistry*, **56(10)**: 2744-2752 (2019).

[79] Soleimani Amiri S., Green Production and Antioxidant Activity Study of New Pyrrolo [2, 1- a] isoquinolines. *J. Heterocyclic Chem.*, **57(11)**: 4057-4069 (2020).

[80] Samiei Z., Soleimani-Amiri S., Azizi Z., Fe3O4@ C@ OSO3H as an Efficient, Recyclable Magnetic Nanocatalyst in Pechmann Condensation: Green Synthesis, Characterization, and Theoretical Study, *Molecular Diversity*, **25(1)**: 67-86 (2021).

[81] Taheri Hatkehlouei S.F., Mirza B., Soleimani-Amiri S., Solvent-free One-Pot Synthesis of Diverse Dihydropyrimidinones/ Tetrahydropyrimidinones Using Biginelli Reaction Catalyzed by Fe_3O_4@ C@ OSO3H, *Polycyclic Aromat. Compd.*, **42(4)**: 1341-1357 (2022).

[82] Amiri S.S., Ghazvini M., Khandan S., Afrashteh S., KF/Clinoptilolite@ MWCNTs Nanocomposites Promoted a Novel Four-Component Reaction of Isocyanides for the Green Synthesis of Pyrimidoisoquinolines in Water, *Polycyclic Aromat. Compd*., **42**: 1-16 (2021).

[83] Zarei F., Soleimani-Amiri S., Azizi Z., Heterogeneously Catalyzed Pechmann Condensation Employing the HFe (SO_4) 2.4 H_2O-Chitosan Nano-Composite: Ultrasound-Accelerated Green Synthesis of Coumarins, Polycyclic Aromat. Compd., 1-18 (2021).

[84] Feizpour Bonab M., Soleimani-Amiri S., Mirza B., Fe_3O_4@C@PrS-SO_3H: A Novel Efficient Magnetically Recoverable Heterogeneous Catalyst in the Ultrasound-Assisted Synthesis of Coumarin Derivatives, *Polycyclic Aromat. Compd.*, 1-16 (2022).

[85] Soleimani-Amiri S., Hossaini Z., Azizi Z., Synthesis and Investigation of Biological Activity of New Oxazinoazepines: Application of Fe_3O_4/CuO/ZnO@ MWCNT Magnetic Nanocomposite in Reduction of 4-Nitrophenol in Water, *Polycyclic Aromat. Compd.*, 1-22 (2022).

[86] Khoshtarkib Z., Ebadi A., Alizadeh R., Ahmadi R., Amani V., Dichloridobis (phenanthridine-κN) zinc (II), *Acta Crystallog. E*: **65(7)**: m739-m740 (2009).

[87] Salehi N., Chemical composition of the Essential oil from Aerial parts of Achillea filipendulina Lam. From Iran, *J. Chem. Lett.*, **1**: 160-163 (2020).

[88] Amani V., Ahmadi R., Naseh M., Ebadi A., Synthesis, Spectroscopic Characterization, Crystal Structure and Thermal Analyses of Two Zinc (II) Complexes with Methanolysis of 2-Pyridinecarbonitrile as a Chelating Ligand, *Journal of the Iranian Chemical Society*, **14(3)**: 635-642 (2017).

[89] Iji M., Dass P. M., Shalbugau K. W., Penuel B.L., Synthesis and Characterization of Heterogeneous Catalysts from Magnetic Sand and Kaolin, *Journal of Chemistry Letters*, **1(3)**: 139-142 (2020)

[90] Ahmadi R., Khalighi A., Kalateh K., Amani V., Khavasi H.R., Catena-Poly [[(5, 5′-dimethyl-2, 2′-bipyridine-κ2N, N′) cadmium (II)]-di-μ-chloride], *Acta Crystallog. E*, **64(10)**: m1233-m1233 (2008).

[91] Benhachem F.Z., Harrache D., Evaluation of Physico-Chemical Quality and Metallic Contamination Level of Epikarstic Seepage Waters in Forest Zone, *J. Chem. Lett.*, **1**: 59-62 (2020).

[92] Soleimani- Amiri S., Arabkhazaeli M., Hossaini Z., Afrashteh S., Eslami A. A. Synthesis of Chromene Derivatives via Three- Component Reaction of 4- hydroxycumarin Catalyzed by Magnetic Fe_3O_4 Nanoparticles in Water, *Journal of Heterocyclic Chemistry*, **55(1)**: 209-213 (2018).

[93] Soleimani- Amiri S., Hossaini Z., Arabkhazaeli M., Karami H., Afshari Sharif Abad S. Green Synthesis of Pyrimido- Isoquinolines and Pyrimido- Quinoline Using ZnO Nanorods as an Efficient Catalyst: Study of Antioxidant Activity, *Journal of the Chinese Chemical Society*, **66(4)**: 438-445 (2019).

[94] Norouzi N. Dynamic Modeling of the Effect of Vehicle Hybridization Policy on Carbon Emission and Energy Consumption, *J. Chem. Lett.*, **3**: 99-106(2022).

[95] Soleimani- Amiri S., Hossaini Z., Azizi Z., Synthesis and Investigationof Antioxidant and Antimicrobial Activity of New Pyrazinopyrroloazepine Derivatives Using Fe3O4/CuO/ZnO@MWCNT MNCs as Organometallic Nanocatalyst by New MCRs, *Appl. Organomet. Chem.*, **36(4)**: e6573 (2022).

[96] Karbakhshzadeh A., Majedi S., Abbasi V., Computational Investigation on Interaction Between Graphene Nanostructure BC_3 and Rimantadine Drug, *J. Chem. Lett.*, **3**: 108-113 (2022).

[97] Norouzi N., Ebadi A. G., Bozorgian A., Vessally E., Hoseyni S. J., Energy and Exergy Analysis of Internal Combustion Engine Performance of Spark Ignition for Gasoline, Methane, and Hydrogen Fuels, *Iran. J. Chem. Chem. Eng. (IJCCE)*, **40(6)**: 1909-1930 (2021).

[98] Rabipour S., Mahmood E. A., Afsharkhas M., Abbasi V., Cannabinoids Impact on Cognition: A Review from the Neurobiological Perspective, *Chem. Rev. Lett.*, **6**: 7-14 (2023).

[99] Norouzi N., Ebadi A. G., Bozorgian A., Hoseyni S. J., Vessally E., Cogeneration System of Power, Cooling, and Hydrogen from Geothermal Energy: An Exergy Approach, *Iran. J. Chem. Chem. Eng. (IJCCE)*, **41(2)**: 706-721 (2022).

[100] Silas K., Musa Y.P., Habiba M.D., Effective Application of Jatropha Curcas Husk Activated ZnCl2, *Chem. Rev. Lett.*, **5**: 153-160 (2022).

[101] Khezri A., Edjlali L., Eshaghi M., Vardini M.T., Basharnavaz H., A Novel [3-(4-methoxyphenyl) isoxazole-5-yl]-methanol Compound: Synthesis, *Chem. Rev. Lett.*, **5**: 113-118 (2022).

[102] Hoseyni S.J., Manoochehri M., Asli M.D., Synthesis and Crystal Structure of Dibromido{[(2-Pyridyl) methyl](p-ethylphenyl)amine}Zinc, *Chem. Rev. Lett.*, **5**: 99-105 (2022)..

[103] Kadhim M.M., Mahmood E.A., Abbasi V., Poor Heravi M.R., Habibzadeh S., Mohammadi-Aghdam S., Soleimani-amiri S., Theoretical Investigation of the Titanium—Nitrogen Heterofullerenes Evolved from the Smallest Fullerene, *J. Mol. Graph. Model.*, (2022).

[104] Porgar S., Rahmanian N., Phase equilibrium for hydrate formation in the Methane and Ethane system and effect of inhibitors, *Chem. Rev. Lett.*, **5**: 2-11 (2022).

[105] Kadhim M.M., Mahmood E.A., Abbasi V., Poor Heravi M.R., Habibzadeh S., Mohammadi-Aghdam S., Shoaei S.M., Theoretical Investigation of the Titanium—Nitrogen Heterofullerenes Evolved from the Smallest Fullerene, *J. Mol. Graph. Model.*, **117**: 108269 (2022).

[106] Avşar C., Tümük D., Ertunç S., Gezerman A.O., A Review on Ammono-Carbonation Reactions: Focusing on the Merseburg Process, *Chem. Rev. Lett.*, **5**: 83-91 (2022).

[107] Rabipour S., Mahmood E., Ebadi A., Bozorgian A., Vessally E., Asadi Z., Afsharkhas M., A Systematic Review of Therapeutic Potential of Illicit Drugs: A Narrative Overview of How Cannabinoids and Psychedelics Can be Used in Medicine, *Iran. J. Chem. Chem. Eng. (IJCCE)*, **41(3)**: 722-752 (2022).